

Variational Nonlinear State Estimation*

Jarrad Courts^{†1}, Adrian Wills^{‡2}, and Thomas B. Schön^{§, ¶3}

¹*School of Engineering, University of Newcastle, Australia*

²*School of Engineering, University of Newcastle, Australia*

³*Department of Information Technology, Uppsala University, Sweden*

October 16, 2020

Abstract

In this paper, the problem of state estimation, in the context of both filtering and smoothing, for nonlinear state-space models is considered. Due to the nonlinear nature of the models, the state estimation problem is generally intractable as it involves integrals of general nonlinear functions and probability density functions lacking closed-form solutions. As such, it is common to approximate the state estimation problem. In this paper, we develop a solution based on the variational inference principle, which offers the key advantage of a flexible, but principled, mechanism for approximating the required distributions. Our main contribution lies in a new formulation of the state estimation problem as an optimisation problem, which can then be solved using standard optimisation routines that employ exact first- and second-order derivatives. The resulting state estimation approach involves a minimal number of assumptions and is directly applicable to nonlinear systems with both Gaussian and non-Gaussian probabilistic models. The performance of our approach is demonstrated on several examples; a challenging scalar system, a model of a simple robotic system, and a target tracking problem using a von Mises-Fisher distribution and outperforms alternative assumed density approaches to state estimation.

1 Introduction

The problem of state estimation is of great interest to a wide variety of practical scientific and engineering problems [1]. It consists of processing noisy measurements using probabilistic models to describe observed measurements and a related underlying state. The state estimation problem occurs as a filtering problem, and as a smoothing problem.

In this paper the state estimation problem for discrete-time nonlinear state-space models is considered. The model structure consists of two components, a transition model, and a measurement model. These are represented as

$$x_{k+1} \sim p_\theta(x_{k+1} | x_k), \quad (1a)$$

$$y_k \sim p_\theta(y_k | x_k), \quad (1b)$$

respectively, where $\theta \in \mathcal{R}^{n_\theta}$ is a vector of model parameters, $x_k \in \mathcal{R}^{n_x}$ is the state at time k , and $y_k \in \mathcal{R}^{n_y}$ is the observed measurement at time k . Whilst we do consider the presence of an input $u_k \in \mathcal{R}^{n_u}$ throughout this paper it does not influence the approach, as such the notation has been suppressed for clarity.

Given a sequence of $T > 0$ measurements denoted as $y_{1:T} = \{y_1, \dots, y_T\}$ and a prior distribution $p(x_0)$ on the initial state x_0 , we are concerned with both the filtering problem of obtaining $p_\theta(x_k | y_{1:k})$, and the smoothing problem of obtaining each pairwise smoothed distribution, $p_\theta(x_k, x_{k+1} | y_{1:T})$ for $k \in 0, \dots, T-1$. Both of these state estimation problems can be performed recursively with the use of Bayes' rule to describe each state as a probability density function [1].

*This work has been submitted to the IEEE for possible publication. Copyright may be transferred without notice, after which this version may no longer be accessible.

[†]Jarrad.Courts@uon.edu.au

[‡]Adrian.Wills@newcastle.edu.au

[§]thomas.schon@it.uu.se

[¶]This research was financially supported by the Swedish Foundation for Strategic Research (SSF) via the project *ASSEMBLE* (contract number: RIT15-0012), and via the projects *Learning flexible models for nonlinear dynamics* (contract number: 2017-03807), and *NewLEADS - New Directions in Learning Dynamical Systems* (contract number: 621-2016-06079), both funded by the Swedish Research Council.

Generally, models of practical interest are nonlinear and as such direct application of Bayes' rule is intractable. One reason is that the state distributions lack closed-form expressions, another is the requirement to calculate integrals of general nonlinear functions [1, 2].

Variational inference (VI) [3, 4] is a method of approximating posterior distributions with a parametric density of an assumed form. The aim of VI is to find the optimal distribution, as measured by a Kullback-Leiber (KL) divergence [5], of the selected family by recasting the inference problems into optimisation problems [4].

The contribution of this paper is to present a variational inference approach to state estimation for nonlinear discrete-time state-space models; the specific example of utilising a Gaussian assumed density is detailed. Differing from existing work the presented approach relies upon standard optimisation routines that employ exact gradients and exact Hessian's to address both the filtering and smoothing problems; due to the selected parametrisation, this can be efficiently performed. Additionally, the state estimation approach uses a minimal number of assumptions and is directly applicable to both Gaussian and non-Gaussian nonlinear systems. The performance and robustness of the proposed method is demonstrated on several examples. We have partially presented the approach detailed in the unpublished work of [6].

The remainder of this paper is organised as follows; Section 2 provides a brief overview of related work followed by Section 3 detailing the proposed state estimation approach for both filtering and smoothing. Section 4 then provides implementation-specific details followed by numerical examples in Section 5. Section 6 concludes the paper.

2 Related Work

While particle filters [2] and particle smoothers [7] directly handle both the filtering and smoothing problems for nonlinear models they can be computationally costly and alternative, assumed density, approaches are widely used.

Amongst the most popular of these are the extended Kalman filter (EKF) [8], the unscented Kalman filter (UKF) [9], and the respective approaches to smoothing, the extended Kalman smoother (EKS) [10], and the unscented Rauch-Tung-Striebel smoother (URTSS) [11]. These are Gaussian assumed density approaches based upon the Kalman filter [12] and Rauch-Tung-Striebel (RTS) [13] smoothers, which exactly solve the corresponding state estimation problems for linear systems with additive Gaussian noise models.

These approaches function by approximating the nonlinear models about the state prior [14]. Iteratively re-computing this approximation using the posterior distribution, however, can improve the performance [14]. Many iterated EKF and UKF based approaches exist, the iterated posterior linearization filter (IPLF) [14] and the iterated approaches to the UKF in [15] are two examples. The iterated posterior linearization smoother (IPLS) [16] extends this approach to the smoothing problem which is then further generalised in [17] to allow for non-Gaussian models.

All these approaches, however, are based upon a Kalman filtering framework [14]. This limits the form of the state corrections and, for nonlinear models, can be outperformed using alternative approaches [18]. The minimum divergence filter (MDF) [18] is one such approach that is derived from a KL divergence perspective. The MDF, however, is non-iterative and can perform poorly with small measurement noise which can require the artificial introduction of noise [18]. The stochastic search Kalman filter (SKF) [19] is another assumed Gaussian filter based upon minimisation of a KL divergence. The SKF, based upon using Monte-Carlo search, was however found to be outperformed by a moment matching approach.

This KL divergence basis is also known as variational inference. VI has also been used in [20] to provide a variational iterated filter (VIF) and in [21, 22, 23, 24] to perform smoothing of stochastic differential equations. More recently, exactly sparse Gaussian variational inference (ESGVI) [25] has been presented, which is a batch state estimation method for nonlinear systems with a focus on simultaneous localisation and mapping (SLAM), derivative-free methods, and the derivation of an optimiser based upon approximations to first- and, some, second-order derivatives.

A key difference between these related works and our approach is *where* and *when* approximations are introduced and handled. In this paper, only one assumption (selected density form) and one approximation (Gaussian quadrature of integrals) is introduced, and only when required to result in a tractable optimisation problem. The resulting optimisation problem is of standard form and directly solved without any further simplifications using exact first and second-order derivatives to a local maximum; due to the careful parametrisation of the problem these derivatives can be readily calculated.

Contrarily, many of the related works, in particularly the Kalman based approaches, implicitly introduce many

inherited assumptions not necessarily appropriate, or justified, for nonlinear systems. Secondly, and perhaps more importantly, is how the iterations, or optimisation, is performed for both the Kalman and VI based approaches. Generally speaking, the approaches taken can be seen as 'ad-hoc', incorporating *some* of ideas from Newton style optimisation but do not necessarily form efficient and robust optimisation produces such as those detailed in standard optimisation literature such as [26]. This may lead to convergence difficulties or even divergence, a problem observed in many of the iterated approaches. Furthermore, in the development of these optimisation approaches additional simplifications or approximations of the gradient are frequently introduced. The use of second-order derivatives is infrequent; when utilised they are typically approximated, and only for the components relating to the mean, and not the covariance, of the assumed distribution.

3 Variational Nonlinear State Estimation

In this section we first develop the proposed approach to state estimation in the context of smoothing in Section 3.1. The filtering problem is then examined in Section 3.2, which is followed by an illustrative example and discussion in Section 3.3.

3.1 Smoothing

As $p_\theta(x_{0:T} | y_{1:T})$ cannot be represented in closed form it will be approximated using an assumed density, parameterised by β , and denoted as $q_\beta(x_{0:T})$. At a high level, assumed density smoothing consist of two steps; firstly, selecting a tractable parametric form, and secondly, for a given parametric form, obtaining a numeric value for β . For a given parametric form, approaches to assumed density smoothing differ by how the value of β is obtained. In this paper, the value of β is obtained using variational inference.

Our approach to obtaining values for β begins by utilising conditional probability to express the log-likelihood, $\log p_\theta(y_{1:T})$, as

$$\log p_\theta(y_{1:T}) = \log p_\theta(x_{0:T}, y_{1:T}) - \log p_\theta(x_{0:T} | y_{1:T}), \quad (2)$$

independent of $q_\beta(x_{0:T})$. The assumed density is introduced by adding and subtracting $\log q_\beta(x_{0:T})$ to the right hand side of (2). With minor rearrangement this leads to

$$\log p_\theta(y_{1:T}) = \log \frac{p_\theta(x_{0:T}, y_{1:T})}{q_\beta(x_{0:T})} + \log \frac{q_\beta(x_{0:T})}{p_\theta(x_{0:T} | y_{1:T})}. \quad (3)$$

As $\log p_\theta(y_{1:T})$ is independent of $x_{0:T}$ we can write

$$\log p_\theta(y_{1:T}) = \int q_\beta(x_{0:T}) \log p_\theta(y_{1:T}) x_{0:T}. \quad (4)$$

By substitution of (3) into the right hand of (4) we arrive at

$$\begin{aligned} \log p_\theta(y_{1:T}) &= \int q_\beta(x_{0:T}) \log \frac{p_\theta(x_{0:T}, y_{1:T})}{q_\beta(x_{0:T})} dx_{0:T} \\ &\quad + \int q_\beta(x_{0:T}) \log \frac{q_\beta(x_{0:T})}{p_\theta(x_{0:T} | y_{1:T})} dx_{0:T}, \end{aligned} \quad (5)$$

which is equivalent to

$$\log p_\theta(y_{1:T}) = \mathcal{L}(\beta) + \text{KL}[q_\beta(x_{0:T}) || p_\theta(x_{0:T} | y_{1:T})], \quad (6)$$

where $\text{KL}[q_\beta(x_{0:T}) || p_\theta(x_{0:T} | y_{1:T})]$ is the KL divergence of $p_\theta(x_{0:T} | y_{1:T})$ from $q_\beta(x_{0:T})$ and

$$\mathcal{L}(\beta) = \int q_\beta(x_{0:T}) \log \frac{p_\theta(x_{0:T}, y_{1:T})}{q_\beta(x_{0:T})} dx_{0:T}. \quad (7)$$

As $\text{KL}[q_\beta(x_{0:T}) || p_\theta(x_{0:T} | y_{1:T})] \geq 0$, from (6), it is seen that

$$\log p_\theta(y_{1:T}) \geq \mathcal{L}(\beta) \quad (8)$$

and hence $\mathcal{L}(\beta)$ is a lower bound to the log-likelihood, $\log p_\theta(y_{1:T})$.

The proposed approach to smoothing consists of selecting a value for β , denoted β^* , by maximising this lower bound to the log-likelihood via

$$\beta^* = \arg \max_{\beta} \mathcal{L}(\beta). \quad (9)$$

The resulting smoothed density is then given by $q_{\beta^*}(x_{0:T})$.

The use of (9) to obtain numerical values of β poses several appealing properties. Firstly, no representation of $p_{\theta}(x_{0:T} | y_{1:T})$ is required; this avoids one of the problems associated with the direct use of Bayes' rule to perform smoothing.

Secondly, if the parametric form of $q_{\beta}(x_{0:T})$ matches $p_{\theta}(x_{0:T} | y_{1:T})$ the KL divergence term can be driven to zero by the maximisation. This means $q_{\beta^*}(x_{0:T})$ is identical to $p_{\theta}(x_{0:T} | y_{1:T})$ and smoothing has been performed exactly.

Thirdly, from (6) and due to both the non-negativity of any KL divergence and $\log p_{\theta}(y_{1:T})$ being constant, maximisation of $\mathcal{L}(\beta)$ is equivalent to minimisation of $\text{KL}[q_{\beta}(x_{0:T}) || p_{\theta}(x_{0:T} | y_{1:T})]$. This is the motivation behind maximising $\mathcal{L}(\beta)$, it allows the KL divergence of $p_{\theta}(x_{0:T} | y_{1:T})$ from $q_{\beta}(x_{0:T})$ to be minimised without requiring $p_{\theta}(x_{0:T} | y_{1:T})$.

This overall approach of approximating an intractable inference problem with an optimisation problem is known as variational inference. The VI approach has been utilised in many fields, and a particularly prominent example is the field of machine learning [27].

While (9) avoids $p_{\theta}(x_{0:T} | y_{1:T})$ it remains generally intractable. One reason is that $q_{\beta}(x_{0:T})$ is an assumed density to the full posterior distribution; with an increasing number of time steps, calculations involving the full posterior distribution $p_{\theta}(x_{0:T} | y_{1:T})$, or approximations thereof, will become computationally prohibitive [1]. However, the smoothing problem this paper considers is obtaining assumed density approximations $q_{\beta}(x_k, x_{k+1})$, to each pairwise joint smoothed distribution $p_{\theta}(x_k, x_{k+1} | y_{1:T})$, and not to obtain $q_{\beta}(x_{0:T})$.

To utilise the approach given by (9) it is required to express $\mathcal{L}(\beta)$ as a function of each $q_{\beta}(x_k, x_{k+1})$ rather than $q_{\beta}(x_{0:T})$. To achieve this we begin by separating $\mathcal{L}(\beta)$ as

$$\mathcal{L}(\beta) = \int q_{\beta}(x_{0:T}) \log \frac{p_{\theta}(x_{0:T}, y_{1:T})}{q_{\beta}(x_{0:T})} dx_{0:T} \quad (10a)$$

$$= \int q_{\beta}(x_{0:T}) \log p_{\theta}(x_{0:T}, y_{1:T}) dx_{0:T} - \int q_{\beta}(x_{0:T}) \log q_{\beta}(x_{0:T}) dx_{0:T}. \quad (10b)$$

From conditional probability, and the conditional independence of the measurements, we can write

$$p_{\theta}(x_{0:T}, y_{1:T}) = p(x_0) \prod_{k=0}^{T-1} p_{\theta}(x_{k+1}, y_{k+1} | x_k). \quad (11)$$

This allows $\log p_{\theta}(x_{0:T}, y_{1:T})$ to be written as

$$\begin{aligned} \log p_{\theta}(x_{0:T}, y_{1:T}) &= \log \left(p(x_0) \prod_{k=0}^{T-1} p_{\theta}(x_{k+1}, y_{k+1} | x_k) \right) \\ &= \log p(x_0) + \log \prod_{k=0}^{T-1} p_{\theta}(x_{k+1}, y_{k+1} | x_k) \\ &= \log p(x_0) + \sum_{k=0}^{T-1} \log p_{\theta}(x_{k+1}, y_{k+1} | x_k), \end{aligned}$$

and hence the first integral in (10b) can be expressed as

$$\int q_{\beta}(x_{0:T}) \log p_{\theta}(x_{0:T}, y_{1:T}) dx_{0:T} = I_1 + I_{23}, \quad (12)$$

where

$$I_1 = \int q_\beta(x_{0:T}) \log p(x_0) dx_{0:T}, \quad (13a)$$

$$I_{23} = \int q_\beta(x_{0:T}) \sum_{k=0}^{T-1} \log p_\theta(x_{k+1}, y_{k+1} \mid x_k) dx_{0:T} \quad (13b)$$

$$= \sum_{k=0}^{T-1} \int q_\beta(x_{0:T}) \log p_\theta(x_{k+1}, y_{k+1} \mid x_k) dx_{0:T} \quad (13c)$$

$$= I_2 + I_3, \quad (13d)$$

and

$$I_2 = \sum_{k=0}^{T-1} \int q_\beta(x_{0:T}) \log p_\theta(x_{k+1} \mid x_k) dx_{0:T}, \quad (13e)$$

$$I_3 = \sum_{k=0}^{T-1} \int q_\beta(x_{0:T}) \log p_\theta(y_{k+1} \mid x_{k+1}) dx_{0:T}. \quad (13f)$$

Due to the fact that $p_\theta(x_{k+1} \mid x_k)$ and $p_\theta(y_{k+1} \mid x_{k+1})$ only depend upon a small subset of $x_{0:T}$ and since $q_\beta(x_{0:T})$ is a probability distribution, the dimension of these integrals can be reduced to

$$I_1 = \int q_\beta(x_0) \log p(x_0) dx_0, \quad (14a)$$

$$I_2 = \sum_{k=0}^{T-1} \int q_\beta(x_{k:k+1}) \log p_\theta(x_{k+1} \mid x_k) dx_{k:k+1}, \quad (14b)$$

$$I_3 = \sum_{k=0}^{T-1} \int q_\beta(x_{k+1}) \log p_\theta(y_{k+1} \mid x_{k+1}) dx_{k+1}. \quad (14c)$$

This simplifies the calculation of the lower bound to

$$\mathcal{L}(\beta) = \int q_\beta(x_{0:T}) \log \frac{p_\theta(x_{0:T}, y_{1:T})}{q_\beta(x_{0:T})} dx_{0:T} \quad (15a)$$

$$= I_1 + I_2 + I_3 - I_4, \quad (15b)$$

where

$$I_4 = \int q_\beta(x_{0:T}) \log q_\beta(x_{0:T}) dx_{0:T}, \quad (16)$$

which can be rewritten (see the Appendix) as

$$I_4 = \sum_{k=0}^{T-1} \int q_\beta(x_{k:k+1}) \log q_\beta(x_{k:k+1}) dx_{k:k+1} - \sum_{k=1}^{T-1} \int q_\beta(x_k) \log q_\beta(x_k) dx_k. \quad (17)$$

From I_1 , I_2 , I_3 , and I_4 it is seen that the calculation of $\mathcal{L}(\beta)$ never requires the full distribution $q_\beta(x_{0:T})$, instead it is just the pairwise joint distributions $q_\beta(x_k, x_{k+1})$ and marginals thereof that are required.

It remains to detail how to address the generally intractable integrals in I_1 , I_2 , I_3 , and I_4 and how to perform the maximisation. While critical from an implementation point of view, these details are conceptually unimportant. As such they are temporarily deferred in favour of examining the application of this approach to a linear system and the minor change required to apply this approach to more general state-space models.

3.1.1 Application to linear and nonlinear systems

Consider a linear state-space model with additive Gaussian noise according to

$$x_{k+1} = Ax_k + Bu_k + v_k, \quad (18a)$$

$$y_k = Cx_k + Du_k + e_k, \quad (18b)$$

where

$$v_k \sim \mathcal{N}(0, Q), \quad e_k \sim \mathcal{N}(0, R), \quad (18c)$$

and the initial state prior is given by $p(x_0) = \mathcal{N}(x_0; \mu_0, P_0)$. The smoothing distribution, $p_\theta(x_{0:T} \mid y_{1:T})$, for this class of systems takes the form of a multivariate Gaussian, the numerical values of which are given by the closed-form Kalman smoothing equations [13].

Now consider the proposed smoothing approach applied to this linear system. First a form for $q_\beta(x_{0:T})$ must be selected, here we chose to use a multivariate Gaussian. This implies that $q_\beta(x_{0:T})$ and $p_\theta(x_{0:T} \mid y_{1:T})$ have the same functional form, which in turn means that there exists some β^* such that $q_{\beta^*}(x_{0:T})$ is identical to $p_\theta(x_{0:T} \mid y_{1:T})$. For this β^* we have that

$$\text{KL}[q_{\beta^*}(x_{0:T}) \parallel p_\theta(x_{0:T} \mid y_{1:T})] = 0, \quad (19)$$

and therefore

$$\log p_\theta(y_{1:T}) = \mathcal{L}(\beta^*). \quad (20)$$

As $\mathcal{L}(\beta)$ is a lower bound to $\log p_\theta(y_{1:T})$ this implies that β^* can be found via

$$\beta^* = \arg \max_{\beta} \mathcal{L}(\beta), \quad (21)$$

where, due to the system being linear, the integrals within $\mathcal{L}(\beta)$ have a tractable closed-form solution and the resulting distribution $q_{\beta^*}(x_{0:T})$ will match the Kalman smoothed solution. This occurs due to the fact that $q_\beta(x_{0:T})$ is sufficiently flexible to exactly match $p_\theta(x_{0:T} \mid y_{1:T})$ and the maximisation has indeed driven any difference between these distributions to zero.

We now progress to consider the application of this smoothing approach to general nonlinear state-space models in the form of (1) with the continued assumption that each $q_\beta(x_k, x_{k+1})$ is a multivariate Gaussian distribution. Compared with application to a linear system, this has two important consequences.

Firstly, as true for all assumed density approaches to state estimation, $q_\beta(x_{0:T})$ will, generally, not be able to exactly match $p_\theta(x_{0:T} \mid y_{1:T})$. As such the KL divergence term will remain strictly positive and $\mathcal{L}(\beta)$ will not equal $\log p_\theta(y_{1:T})$ in general.

The second, more influential, consequence is that $\mathcal{L}(\beta)$ becomes intractable to compute due to the general nonlinear integrals within I_2 and I_3 . Since evaluation of these integrals is necessary they will be numerically approximated, the approximations to I_2 , I_3 , and hence $\mathcal{L}(\beta)$ are given by \hat{I}_2 , \hat{I}_3 , and $\hat{\mathcal{L}}(\beta)$ respectively. As the optimisation problem of (9) is intractable it is replaced by

$$\begin{aligned} \beta^* &= \arg \max_{\beta} \hat{\mathcal{L}}(\beta) \\ &= \arg \max_{\beta} I_1 + \hat{I}_2 + \hat{I}_3 - I_4. \end{aligned} \quad (22)$$

This approach to smoothing requires only one minor adaptation when applied to the more general class of nonlinear state-space models given by (1) as opposed to linear systems. This singular difference is that an integral must be numerically approximated rather than calculated in closed form.

3.1.2 Tractable Gaussian Assumed Density Smoother

In this section, a parametrisation of the assumed state distribution is detailed. The given parametrisation is selected as it allows (22) to become a tractable optimisation problem with readily obtainable first- and second-order derivatives. The resulting optimisation problem is in a form that can be directly handled by standard nonlinear programming routines.

Each joint normally distributed assumed density will be represented by

$$q_{\beta_k}(x_k, x_{k+1}) = \mathcal{N}\left(\begin{bmatrix} x_k \\ x_{k+1} \end{bmatrix}; \begin{bmatrix} \mu_k \\ \bar{\mu}_k \end{bmatrix}, P_k^{\frac{T}{2}} P_k^{\frac{1}{2}}\right), \quad (23)$$

where $\mu_k \in \mathcal{R}^{n_x \times 1}$, $\bar{\mu}_k \in \mathcal{R}^{n_x \times 1}$, and $P_k^{\frac{1}{2}} \in \mathcal{R}^{2n_x \times 2n_x}$ describe the joint state distribution and

$$P_i^{\frac{1}{2}} = \begin{bmatrix} A_i & B_i \\ 0 & C_i \end{bmatrix}, \quad (24)$$

where $A, B, C \in \mathcal{R}^{n_x \times n_x}$ and A, C are upper triangular. The parameters in β_k are now given as

$$\beta_k = \{\mu_k, \bar{\mu}_k, A_k, B_k, C_k\}, \quad (25)$$

and they are related to β by

$$\beta = \{\beta_1, \beta_2, \dots, \beta_T\}. \quad (26)$$

Furthermore, we have to ensure that the marginal distribution $q_{\beta}(x_k)$ is the same independently of if it is calculated from $q_{\beta}(x_{k-1}, x_k)$ or $q_{\beta}(x_k, x_{k+1})$. This is expressed by the constraints

$$\mu_{i+1} - \bar{\mu}_i = 0, \quad (27a)$$

$$\text{vech}(B_i^T B_i + C_i^T C_i) - \text{vech}(A_{i+1}^T A_{i+1}) = 0, \quad (27b)$$

for $i \in 1, \dots, T-1$ where $\text{vech}(X)$, defined in [28], stacks the distinct elements of the symmetric matrix X .

The important property of this parametrisation is that the Cholesky decomposition, $P_i^{\frac{1}{2}}$, of each joint distribution is directly available from β_k . This allows the approximations \hat{I}_2 and \hat{I}_3 to be easily approximated using a Gaussian quadrature as

$$\hat{I}_2 = \sum_{j=1}^{n_s} w_j \log p(x_{k+1}^j | x_k^j), \quad (28a)$$

$$\hat{I}_3 = \sum_{j=1}^{n_s} w_j \log p(y_{k+1} | x_{k+1}^j), \quad (28b)$$

where w_j is a weight, and the n_s sigma points are denoted as $\bar{x}^j \in \mathcal{R}^{2n_x \times 1}$ where $\bar{x}^j = \begin{bmatrix} x_k^j \\ x_{k+1}^j \end{bmatrix}$ is given by

linear combinations of the joint mean $[\mu_k^T, \bar{\mu}_k^T]^T$ and the columns of $P_k^{\frac{T}{2}}$. The sigma points, \bar{x}^j , being linear combinations of the elements of β_k are important as they significantly simplify the calculation of both first- and second-order derivatives used in the optimisation.

The likelihood lower bound $\mathcal{L}(\beta)$ can now be approximated by $\hat{\mathcal{L}}(\beta)$ as

$$\hat{\mathcal{L}}(\beta) = I_1 + \hat{I}_2 + \hat{I}_3 - I_4, \quad (29a)$$

where

$$\begin{aligned} I_1 &= -\frac{n_x}{2} \log 2\pi - \sum_{i=1}^{n_x} \log P_0^{\frac{1}{2}}(i, i) - \frac{1}{2} \text{tr}(P_0^{-1} A_1^T A_1) \\ &\quad - \frac{1}{2} \left(P_0^{-\frac{T}{2}} (\mu_0 - \mu_1) \right)^T \left(P_0^{-\frac{T}{2}} (\mu_0 - \mu_1) \right), \end{aligned} \quad (29b)$$

$$\hat{I}_2 = \sum_{k=1}^T \sum_{j=1}^{n_s} w_j \log p(x_{k+1}^j | x_k^j), \quad (29c)$$

$$\hat{I}_3 = \sum_{k=1}^T \sum_{j=1}^{n_s} w_j \log p(y_{k+1} | x_{k+1}^j), \quad (29d)$$

$$\begin{aligned} I_4 &= -\frac{(T+1)n_x}{2} \log 2\pi - \frac{(T+1)n_x}{2} \\ &\quad - \sum_{k=1}^T \sum_{i=1}^{n_x} \log C_k(i, i) - \sum_{i=1}^{n_x} \log A_1(i, i). \end{aligned} \quad (29e)$$

Algorithm 1 Smoothing

Input: Measurements $y_{1:T}$, prior mean μ_0 and covariance P_0 , initial estimate of β

Output: Smoothed distributions $q_{\beta_{k+1}^*}(x_k, x_{k+1})$ for $k \in 0, \dots, T-1$

- Obtain β^* from (30) initialised at β

- $\{\beta_1^*, \beta_2^*, \dots, \beta_T^*\} = \beta^*$

Algorithm 2 Filtering

Input: Measurement y_1 , prior mean μ_0 and covariance P_0 , initial estimate of β

Output: Filtered distribution $\mathcal{N}(x_1; \bar{\mu}_1, B_1^T B_1 + C_1^T C_1)$

- Obtain β^* using Algorithm 1 with $T = 1$ initialised at β

- Extract $\bar{\mu}_1$, B_1 , and C_1 from β^*

Here, the notation $X(i, i)$ refers to the i^{th} diagonal element of X .

The proposed approach to assumed density smoothing for nonlinear models of the class (1) is now tractably given by performing

$$\beta^* = \arg \max_{\beta} \hat{\mathcal{L}}(\beta) \quad \text{s.t.} \quad (27). \quad (30)$$

This constrained optimisation problem is of a standard form and can be directly solved using standard nonlinear programming routines. This optimisation is robustly performed without introducing any further approximations, to a local maximum, utilising exact first- and second-order derivatives.

The assumed density approximation to each pairwise smoothed joint distribution are given by $q_{\beta_{k+1}^*}(x_k, x_{k+1})$ for $k \in 0, \dots, T-1$ where

$$\{\beta_1^*, \beta_2^*, \dots, \beta_T^*\} = \beta^*. \quad (31)$$

The resulting smoother is summarised in Algorithm 1.

3.2 Filtering

In this section one step of the recursive assumed density filtering problem is considered. That is, given an assumed Gaussian density for the previous time step, $p(x_0) = \mathcal{N}(x_0, \mu_0, P_0)$, and the measurement for the current time step, y_1 , compute a Gaussian approximation of $p(x_1 | y_1)$.

As this is a special case of the smoothing problem with $T = 1$ the proposed approach to filtering consists of two steps. Firstly, perform smoothing with a single measurement. Secondly, marginalise the resultant joint distribution to obtain a Gaussian approximation of $p(x_1 | y_1)$. Algorithm 2 provides the proposed approach to filtering and results in unconstrained optimisation problems.

3.3 Illustrative Example and Discussion

In this section, we discuss the properties of the proposed approach to state estimation and how it compares to existing alternative approaches to state estimation. In order to do this we make use of an illustrative example where the proposed state estimation approach is used to make one correction step. To this end, we consider the following measurement model

$$y = 0.01x|x| + e, \quad e \sim \mathcal{N}(0, 0.1), \quad (32)$$

with a prior of $\mathcal{N}(0, 0.4)$ and an observed measurement of $y = 15$.

Fig. 1 shows the resulting state distribution for the proposed approach, the IPLF with 50 iterations (IPLF-50), and a numerically evaluated ground truth. As seen, the IPLF is overconfident while the proposed approach provides a good approximation of the true posterior. This difference is due to the fact that the IPLF is based upon a Kalman

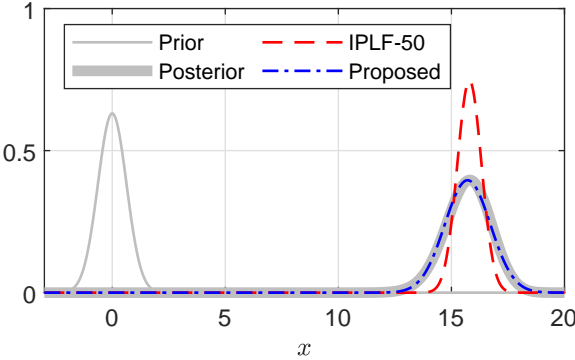


Figure 1: Comparison of state correction approaches illustrating a limitation of using Kalman based corrections for nonlinear measurement models. The Kalman correction based IPLF-50 is overconfident while the proposed method, which is not limited to linear corrections, closely matches the true posterior.

filtering framework which limits the corrections steps to linear corrections [18]. The proposed approach has no such limitations.

While Fig. 1 only shows the results for one specific prior and one specific observed measurement, many others—using a variety of measurement models—were tested with the general behaviour remaining consistent with the specific example provided here. During this process, convergence issues were frequently observed for the IPLF. While this issue is acknowledged and addressed in [29] it highlights a potential problem that these iterated approaches may suffer from. There has been a fair bit of work addressing these convergence issues for a variety of iterated filters, see e.g. [30, 31, 15]. Generally, these function by introducing a variety of safeguards, damping, line-searches, and Levenberg-Marquardt based approaches to improve convergence.

Fortunately, the ideas behind these approaches are well established in the extensive quantity of numerical optimisation literature such as [26] and included in all standard optimisation routines. A result of this is that the proposed state estimation approach requires no further considerations regarding convergence.

This highlights a *significant difference* of the proposed approach compared to existing alternatives; namely the posing of the state estimation problem as a standard optimisation problem. By posing the state estimation problem as an optimisation problem the goal of the approach, maximising a lower bound of the log-likelihood, is cleanly *separated* from specific details of the selected optimisation routine.

Due to this, contrary to alternatives such as [29, 14, 16], the proposed approach has no tuning parameters. Instead, the optimisation required is run until convergence to a local maximum.

4 Implementation

In this section, the implementation-specific details of the proposed state estimation approach are presented. Section 4.1 examines the selected form of Gaussian quadrature utilised, Section 4.2 address the calculation of derivatives required for efficient optimisation, and Section 4.3 deals with how each optimisation problem has been initialised.

4.1 Integration

As commonly performed in Gaussian assumed density state estimation we have utilised a third-order unscented transform [9, 32] with $\alpha = 1$, $\kappa = 0$, and $\beta = 0$ to perform the Gaussian quadrature approximations required in all sigma-point methods utilised. While this has worked well for the examples considered higher-order methods, such as those examined in [33], could be utilised if desired at the trade-off of an additional computational cost.

4.2 Derivatives

To efficiently solve the resulting optimisation problem exact first- and second-order derivatives have been utilised. Due to the assumed Gaussian distribution, the derivatives of I_1 and I_4 are available in closed-form. The remaining terms \hat{I}_2 and \hat{I}_3 , containing general nonlinear functions, are not as straightforward. Fortunately, due to the careful parametrisation of each Gaussian to ensure that the sigma points are linear combinations of the variables that are

optimised, exact gradients and exact Hessians can be obtained *without any manual effort*. Standard automatic differentiation tools can be used for this, we have utilised CasADi [34].

For smoothing, the number of variables and the Hessian dimension continues to grow with the number of measurements. However, due to the sparse block diagonal structure of the Hessian, this is not problematic as both the formation and subsequent decomposition of the Hessian possess a linear in time complexity with respect to the number of measurements.

4.3 Initialisation

General nonlinear constrained optimisation problems are central to the proposed state estimation approach. This implies that the initialisation of each optimisation impacts the run-time required to reach a local minimum and, potentially, the obtained solution. In the section, we examine options for initialising the optimisation problems.

The optimisation that arises from the filtering procedure in Algorithm 2 requires initialisation with a joint Gaussian distribution over the previous and current time-step. In the numerical examples provided a predicted joint distribution calculated using a sigma point method is utilised and found to work well. Differing initialisations may, however, be preferable in some situations. An example of this is when alternative, faster, methods such as a UKF perform well. That solution can then be used as an initialisation for the proposed method and may reduce the number of iterations required to converge.

For the smoothing problem, the initialisation consists of providing an initial estimate to each pairwise joint Gaussian distribution, as optimisation routines do not require this point to satisfy the constraints there is significant flexibility regarding how these can be selected. In some situations, problem-specific knowledge can be used to obtain an initial point. More generally initialising the smoother using each of the joint distributions produced by a filtering pass has been found to work well. The examples in Section 5 use both of these approaches to initialise.

Due to the general nonlinear nature of these optimisation problems, it is not possible to provide guarantees or useful quantitative guidelines regarding the selection of the initial points to avoid reaching potentially undesirable and differing local minima. During development, however, both the proposed filtering and smoothing approaches have consistently appeared robust with respect to the initialisation with the use of an ill-defined, "reasonable" initial point.

5 Numerical Examples

In this section, we present three numerical examples where the proposed approach to state estimation is profiled; a challenging scalar system (Section 5.1), a problem representative of a simple robotic system (Section 5.2), and a target tracking example using a von Mises-Fisher distribution (Section 5.3).

We have also used the proposed approach to estimate the states of randomly generated multi-dimensional linear systems with each optimisation randomly initialised. All filtered states, smoothed states, and likelihood calculations matched the results obtained using the Kalman filtering and smoothing equations.

In all examples, the optimisation problems within the proposed approach are run to convergence to a feasible local maximum subject to an optimality tolerance of 1×10^{-10} using fmincon [35]. The exception to this is the smoothing problem in Section 5.2.2, where an alternative trust region solver with an improved rate of convergence, subject to the same tolerance, is used.

5.1 Nonlinear Scalar System

In this example we consider 50 time steps of the following nonlinear system

$$x_{k+1} = 0.9x_k + 10 \frac{x_k}{1 + x_k^2} + 8 \cos(1.2k) + v_k, \quad (33a)$$

$$y_k = 0.05x_k^2 + e_k, \quad (33b)$$

where $v_k \sim \mathcal{N}(0, 1)$, $e_k \sim \mathcal{N}(0, 1)$ and $x_0 \sim \mathcal{N}(5, 4)$. This is identical to the setup that was used in [16] where the IPLS idea was profiled. It is well-known to be a challenging state estimation problem possessing multi-modal state distributions.

For this system, we will compare the performance of the URTSS, IPLS, and our proposed smoother. The proposed smoother was initialised with the proposed filter. For the IPLS one filter and 50 smoothing iterations, denoted

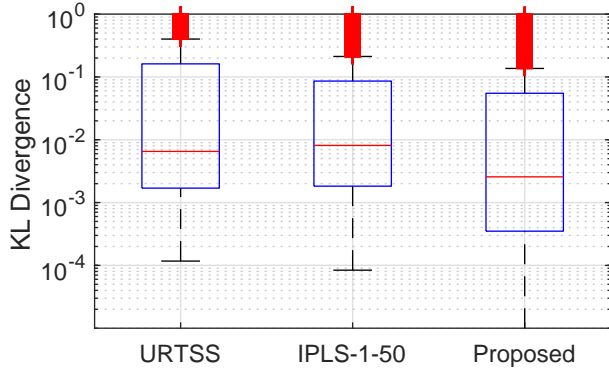


Figure 2: Box plot of the KL divergence between the marginal smoothed state distributions and the grid based ground truth for 100 realisations of system (33), each with 50 time-steps.

IPLS-1-50, were used. As per [16], using one filter iteration with many smoothing iterations performs best on this system.

The performance of these methods is ideally compared using the KL divergence from the true smoothed distribution at each time-step, $\text{KL}[p_\theta(x_k \mid y_{1:T}) \parallel q_\beta(x_k)]$. Since $p_\theta(x_k \mid y_{1:T})$ is intractable we use a very accurate discrete approximation using a fine grid to implement the recursive Bayesian smoothing equations [36]. The KL divergence from this grid based solution is then used to evaluate each assumed density approach.

A box plot [37] of this KL divergence at each time-step for 100 different realisations of (33) with an initial state of $x = 5$ is shown in Fig. 2. The consistently lower KL divergence achieved by the proposed smoother shows it has outperformed the alternative methods.

This improvement has come at the cost of additional run-time with the median run-times for the URTSS, IPLS-1-50, and the proposed smoother being 4.4 ms, 257.5 ms, and 703.5 ms respectively. The proposed smoother required a median of 15 and a maximum of 53 optimisation iterations to converge.

In this example, we have considered a challenging system that possesses non-Gaussian and multi-modal true smoothed state distributions. Due to these properties it cannot be expected that any Gaussian assumed density approach perform well at every time step. Despite this, we have demonstrated that the proposed smoothing method outperforms alternative assumed Gaussian approaches.

5.2 Robot Example

In this example, we consider a continuous-time model of a two-wheeled robot given by

$$\begin{bmatrix} \dot{q}_1(t) \\ \dot{q}_2(t) \\ \dot{q}_3(t) \\ \dot{p}_1(t) \\ \dot{p}_2(t) \end{bmatrix} = \begin{bmatrix} \frac{\cos(q_3(t))p_1(t)}{m} \\ \frac{\sin(q_3(t))p_1(t)}{m} \\ \frac{p_2(t)}{J+ml^2} \\ \frac{-r_1p_1(t)}{m} - \frac{mlp_2^2(t)}{(J+ml^2)^2} + u_1(t) + u_2(t) \\ \frac{(lp_1(t)-r_2)p_2(t)}{J+ml^2} + au_1(t) - au_2(t) \end{bmatrix}, \quad (34)$$

where $r_1 = 1$, $r_2 = 1$, $a = 0.5$, $m = 5$, $J = 2$, $l = 0.15$, $u_1(t)$ is the force applied to the left wheel, $u_2(t)$ is the force applied to the right wheel, and the state vector $x(t) = [\dot{q}_1(t), \dot{q}_2(t), \dot{q}_3(t), \dot{p}_1(t), \dot{p}_2(t)]^T$ consists of x-position, y-position, heading, linear momentum, and angular momentum states respectively. A 50 s simulated trajectory is generated using an ODE solver disturbed by noise sampled from $\mathcal{N}(0, Q)$ where $Q = \text{diag}([0.001, 0.001, 1.745 \times 10^{-3}, 0.001, 0.001])$ at 0.1 s intervals. Measurements at each interval are obtained according to

$$y_k = [q_1(t), q_2(t), q_3(t)]^T + e_k, \quad (35a)$$

$$e_k \sim \mathcal{N}(0, R), \quad (35b)$$

where $R = \text{diag}([0.1^2, 0.1^2, 0.0349^2])$.

The problem of state estimation in the presence of model mismatch is now examined using an Euler discretisation for each 0.1 s interval. Whilst the Euler discretisation introduces some model mismatch the mismatch is primarily due

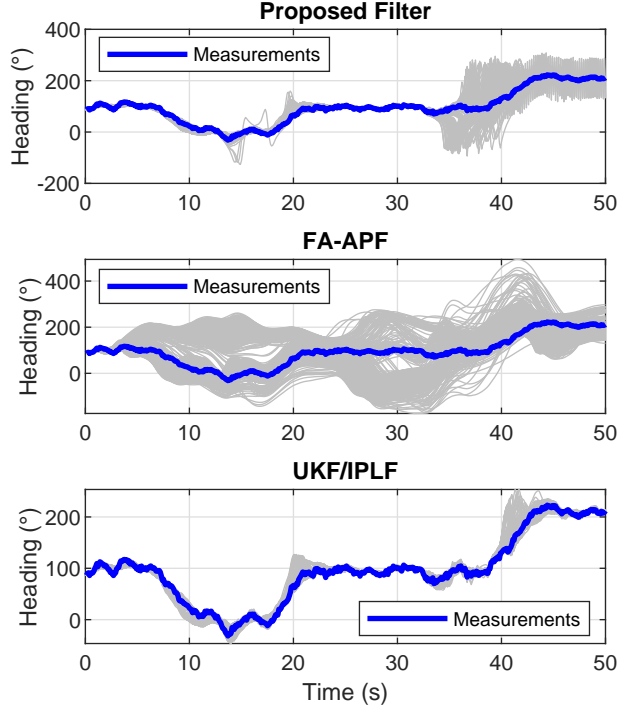


Figure 3: Estimated heading mean for each successful run of the proposed filter, the FA-APF with 5000 particles, and the UKF/IPLF.

to performing the state estimation with the process noise incorrectly given by $Q = \text{diag}([0.01^2, 0.01^2, 0.0035^2, 0.01^2, 0.01^2])$ and m , J , and l randomly given according to

$$m \sim \mathcal{U}(15, 50), \quad J \sim \mathcal{U}(0.01, 1), \quad l \sim \mathcal{U}(0.01, 5).$$

As the measurement model is linear typical iterated Kalman based filters that separate the prediction and correction steps, such as the IPLF, simplify to a UKF. Contrarily, the proposed approach, which does not have separate prediction and correction steps, remains capable of iterating on this system. While alternative approaches to filtering, such as the L-scan IPLF [16] which performs smoothing over the last L measurements, exist and could iterate despite the linear measurement model they are outside of the scope of the filters considered in this paper. Only recursive filters which, given a prior from the previous time-step and a singular observed measurement produce a posterior, are considered.

5.2.1 Filtering

The filtering problem using one set of observed measurements and 500 random sets of mismatched parameters sampled as detailed above are examined. Due to the model mismatch, the robustness of different filtering approaches is primarily of interest for this example. The proposed filter, a fully adapted auxiliary particle filter (FA-APF) [38] with 5000 particles, and a UKF/IPLF (identical for this system) are considered.

The UKF/IPLF—with a square root implementation—was found to be the least robust, diverging 280 of the 500 runs, whereas the FA-APF and the proposed filter diverged only one time each. In Fig. 3 the estimated heading means for each successful run are shown. Despite only diverging once, the state estimates produced by the FA-APF are much less consistent than the proposed method. Fig. 4 shows that the average number of iterations required for convergence at each time step has remained small for the proposed method. The proposed filter required an average of 3.379s to complete all 500 time-steps, when successful the UKF/IPLF required an average of 0.024s.

In this example, we have shown that, at least for this system, the proposed filtering approach is significantly more robust than the UKF/IPLF and has delivered more consistent results than a particle filter. Compared to the successful runs of the UKF/IPLF this has come at the cost of run-time.

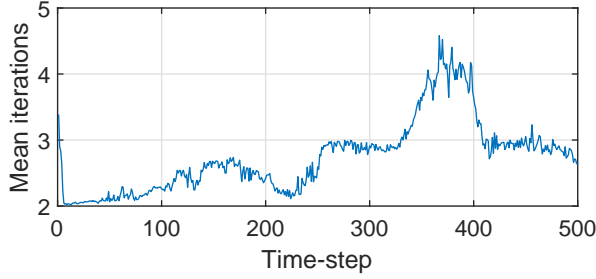


Figure 4: Average number of iterations required for convergence for the proposed filtering method.

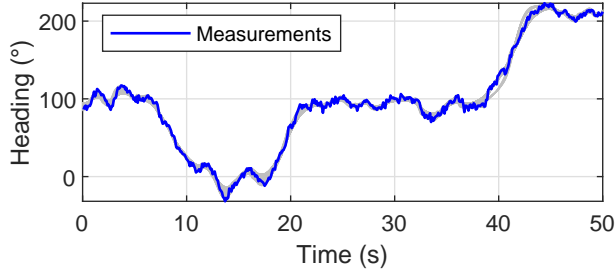


Figure 5: Heading mean for each of the 200 runs of the proposed smoother.

5.2.2 Smoothing

Smoothing on the first 200 trials considered for the filtering example is now considered using both the proposed smoother and the IPLS with one filter iteration and 50 smoothing iterations, denoted IPLS-1-50. To highlight the flexibility of the proposed smoother the state means are initialised using the observed measurements for the first three states and zeros for momentum states. The joint state covariance for each time-step is initially given by $0.01^2 I_{10}$.

The IPLS was unsuccessful 109 times of the 200 attempts; this is due to the first step of the IPLS consisting of a UKF which diverged. Contrarily, the proposed smoother was successful in every run, including the one set of parameters which caused the filter to diverge. Fig. 5 shows the heading mean of each of the 200 runs. As expected, these results are both closer to the observed measurements and more consistent than the estimates produced when filtering in Fig. 3. The proposed smoother required a median of 69 optimisation iterations taking a mean of 35.68 s.

The 81 successful runs of the IPLS, however, required an average of 3.513 s and produced very similar smoothed states as the proposed method. Due to the linear measurement model, this similarity is unsurprising. The exception is the states for the first few seconds, Fig. 6 shows the smoothed means of each state and illustrates the proposed smoother delivered estimates that are more consistent.

The handling of the state prior, $p(x_0)$, is believed to be the cause of this. The IPLS, and indeed all forward-backwards RTS style smoothers, begin with a prediction from the prior for every iteration. This is regardless of the potentially significant difference between the smoothed state estimate for the initial time-step and the prior. While producing the exact smoothing solution for linear systems there does not appear to be any justification for this initial prediction for approximate assumed density smoothers.

Contrarily, the proposed smoother handles the state prior as an expectation using the estimated smoothed state at the initial time-step, at no point is a prediction from the prior performed. This different handling of the prior is how the proposed filtering approach is capable of iterating over both the process and measurement models as opposed to just the measurement model. It is also worth noting that the mean of the state prior matched the true initial state for this example. In situations where the state prior is far from the smoothed state at the initial time-step, the improved handling of the prior would become more pronounced compared with methods that predict from the prior.

In this section, we have demonstrated that the proposed smoothing approach is effective on a multi-dimensional nonlinear system with many time steps. While requiring more run-time than alternatives such as the IPLS the computational cost is not excessive and requires only a moderate amount of iterations to converge. Perhaps more importantly, particularly for the smoothing scenario typically performed offline, is that the proposed smoother

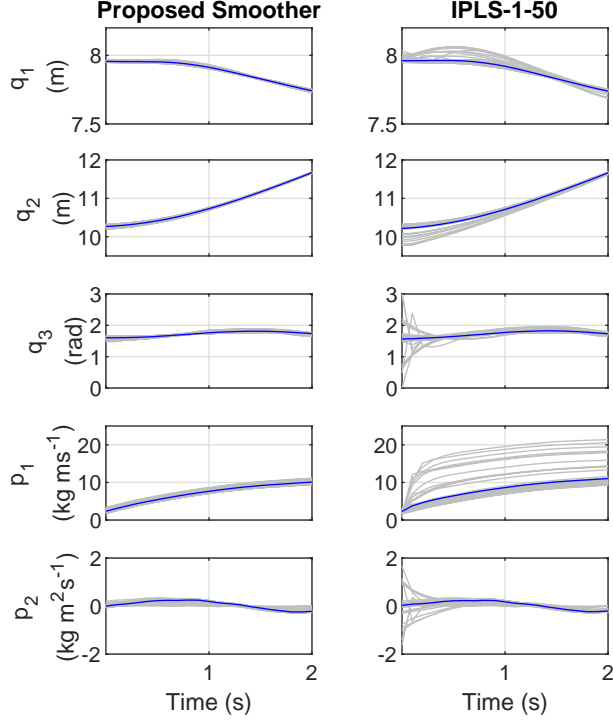


Figure 6: Comparison of the initial smoothed state means using both the proposed smoother (left) and the IPLS-1-50 approach (right) showing that the proposed algorithm is more consistent. Each successful trial is shown in gray, the mean of each successful trial at each time step shown in blue.

appears to be more robust and more consistent than alternative methods.

5.3 Target Tracking Example

In this example we consider a 2-D target tracking problem with a four dimensional state vector, $x = [p_x, v_x, p_y, v_y]^T$, consisting of x and y position and velocity states which is observed using three bearing-only sensors, each modelled using a von Mises-Fisher (VMF) distribution. The process model for this system is given by

$$x_{k+1} = \left(I_2 \otimes \begin{bmatrix} 1 & \tau \\ 0 & 1 \end{bmatrix} \right) x_k + v_k, \quad (36a)$$

$$v_k \sim \mathcal{N} \left(0, q I_2 \otimes \begin{bmatrix} \frac{\tau^3}{2} & \frac{\tau^2}{2} \\ \frac{3}{2} & \tau \end{bmatrix} \right), \quad (36b)$$

where $q = 0.25$, $\tau = 0.5$ and the initial state prior is given by

$$p(x_0) = \mathcal{N}(x_0; \mu_0, \Sigma_0), \quad (37)$$

where $\mu_0 = [-100, 7, 0, 5]^T$, $\Sigma_0 = \text{diag}([20^2, 1, 1, 1])$. The true initial state for each simulation is sampled from this prior. The measurement model for the i^{th} sensor is given by

$$y^i \sim \mathcal{V}(h^i(x), \kappa), \quad (38a)$$

$$h^i(x) = \frac{[p_x - s_x^i, p_y - s_y^i]^T}{\| [p_x - s_x^i, p_y - s_y^i] \|}, \quad (38b)$$

where $\mathcal{V}(h^i(x), \kappa)$ is a VMF distribution with a concentration parameter of $\kappa = 200$ and s_x^i , s_y^i are the x and y positions of the i^{th} sensor, respectively. The three sensors are located at $[100, 0]^T$, $[0, -100]^T$, and $[0, 150]^T$. Throughout this section we consider 100 time steps of this system, an example path with the sensor locations marked is shown in Fig. 7.

This target tracking problem is taken from [39] where, utilising explicit knowledge of moments of the VMF distributions, the IPLF has been extended to produce the VMF-IPLF which has outperformed a variety of alternative

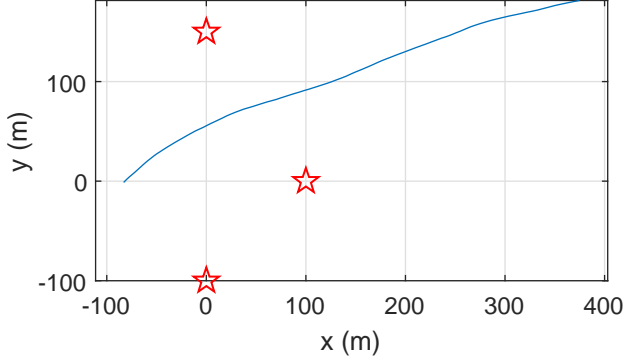


Figure 7: Example path (blue line) used in the target tracking problem with the sensor locations marked by red stars.

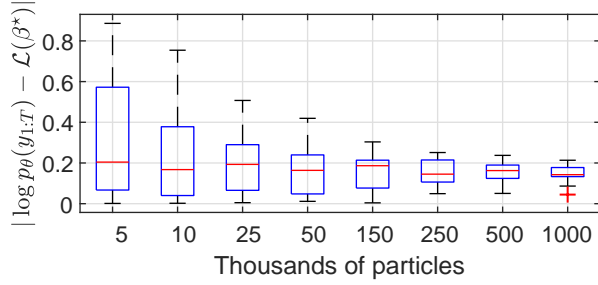


Figure 8: Difference between log-likelihood calculated using a bootstrap particle filter and the proposed filter on a single data-set for a variety of particle counts each performed 20 times.

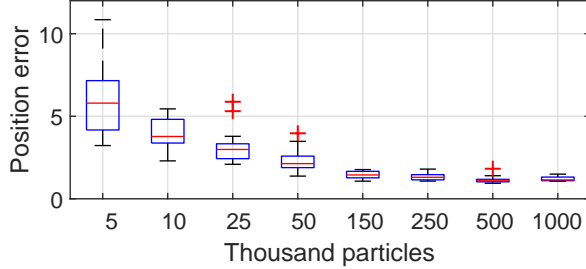


Figure 9: Position error between the state mean calculated using a bootstrap particle filter and the proposed filter on a single data-set for a variety of particle counts each performed 20 times.

Gaussian assumed density filters. We will compare against the sigma point version of the VMF-IPLF with i iterations which we have denoted as VMF-IPLF- i .

To assess the performance of the VMF-IPLF and the proposed filtering approach a bootstrap particle filter (BPF) [2] with many particles is used for comparison. To determine an appropriate quantity of particles we first perform the BPF 20 times on the same data-set with the number of particles ranging from 10^3 to 10^6 . Fig. 8 is a box-plot showing the difference between the log-likelihood calculated from the BPF and the approximate lower bound from the proposed filter for each trial. These results highlight two properties; firstly, the log-likelihood calculated using the BPF and $\mathcal{L}(\beta^*)$ is close, showing that the lower bound is relatively tight. Secondly, as the particle counts continue to increase the improvements of the variance in the BPF start becoming minor at the 500 000 particle mark.

Box-plots showing the position error of the filtered mean of the proposed filter and the VMF-IPLF from the BPF mean for each trial are shown in Fig. 9 and Fig. 10 respectively. These results show that the proposed filter is closer to the particle solution with a large number of particles than the VMF-IPLF.

Fig. 11 shows this position error for 500 different state trajectories using 500 000 particles for the BPF and 50 iterations of the VMF-IPLF. The consistently lower error from the particle solution shows the proposed method has outperformed the VMF-IPLF. As Fig. 12 shows the average number of iteration required to achieve this is quite low. The median run-time to calculate the filtered state trajectories over the 100 time-steps for the VMF-IPLF-50 and the proposed filter are 705 ms and 621 ms respectively, these run-times are close to the time required for the

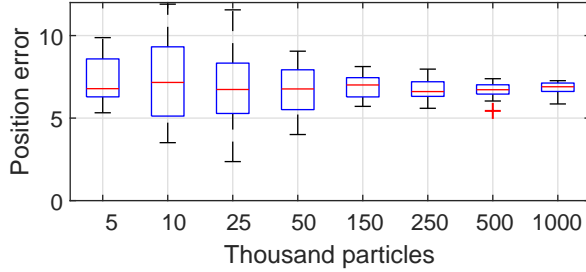


Figure 10: Position error between the state mean calculated using a bootstrap particle filter and the VMF-IPLF on a single data-set for a variety of particle counts each performed 20 times.

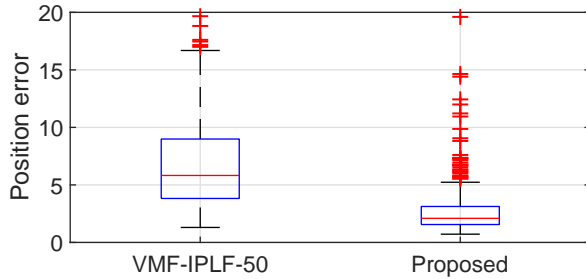


Figure 11: Position error between a BPF solution using 500 000 particles and the VMF-IPLF and the proposed approach over 500 different state trajectories.

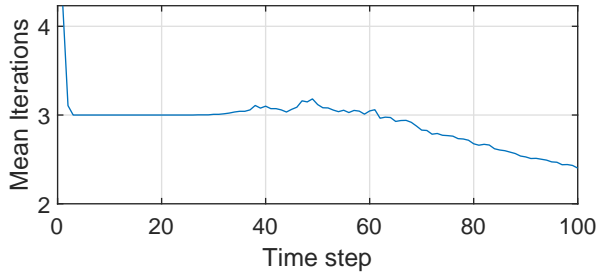


Figure 12: Average iterations required for our proposed filter to converge for each time step of the 500 different trajectories.

BPF with 10 000 particles.

In this section, we have demonstrated the proposed approach to state estimation on a target tracking example using a measurement model with a von Mises-Fisher distribution. This did not require any alterations to the proposed approach to state estimation beyond modifying the log-likelihood calculation. Despite this, we have outperformed an existing approach that has been specifically tailored to a von Mises-Fisher distribution which itself outperformed a variety of assumed density Gaussian filters. This is achieved without significant computational cost, required a minimal number of iterations to converge, and, generally, produced results very close to a particle filter with 500 000 particles.

6 Conclusion

In this paper, we have presented an optimisation based approach to the problem of state estimation for nonlinear and non-Gaussian state-space models using variational inference in the context of both filtering and smoothing. The resulting optimisation problems, of standard form, are efficiently solved using exact first- and second-order derivatives. Several numerical examples have been provided to demonstrate the performance and robustness of the proposed approach compared to alternative methods.

References

[1] S. Särkkä, *Bayesian Filtering and Smoothing*, ser. Institute of Mathematical Statistics Textbooks. Cambridge University Press, 2013.

- [2] N. J. Gordon, D. J. Salmond, and A. F. M. Smith, “Novel approach to nonlinear/non-Gaussian Bayesian state estimation,” *IEE Proceedings F Radar and Signal Processing*, vol. 140, no. 2, p. 107, 1993.
- [3] M. I. Jordan, Z. Ghahramani, T. S. Jaakkola, and L. K. Saul, “An Introduction to Variational Methods for Graphical Models,” *Machine Learning*, vol. 37, no. 2, pp. 183–233, Nov. 1999.
- [4] D. Blei, A. Kucukelbir, and J. McAuliffe, “Variational inference: A review for statisticians,” *Journal of the American Statistical Association*, vol. 112, no. 518, pp. 859–877, 2017.
- [5] S. Kullback and R. A. Leibler, “On Information and Sufficiency,” *The Annals of Mathematical Statistics*, vol. 22, no. 1, pp. 79–86, Mar. 1951.
- [6] J. Courts, C. Renton, T. B. Schön, and A. Wills, “Constructing a variational family for nonlinear state-space models,” 2020.
- [7] A. Doucet, S. Godsill, and C. Andrieu, “On sequential Monte Carlo sampling methods for Bayesian filtering,” *Statistics and Computing*, vol. 10, no. 3, pp. 197–208, 2000.
- [8] A. Jazwinski, *Stochastic processes and filtering theory*. New York: Academic Press, 1970.
- [9] S. J. Julier and J. K. Uhlmann, “New extension of the Kalman filter to nonlinear systems,” in *Signal Processing, Sensor Fusion, and Target Recognition VI*, I. Kadar, Ed. SPIE, Jul. 1997.
- [10] H. Cox, “On the estimation of state variables and parameters for noisy dynamic systems,” *IEEE Transactions on Automatic Control*, vol. 9, no. 1, pp. 5–12, Jan. 1964.
- [11] S. Särkkä, “Unscented Rauch–Tung–Striebel Smoother,” *IEEE Transactions on Automatic Control*, vol. 53, no. 3, pp. 845–849, Apr. 2008.
- [12] R. E. Kalman and R. S. Bucy, “New Results in Linear Filtering and Prediction Theory,” *Journal of Basic Engineering*, vol. 83, no. 1, pp. 95–108, mar 1961.
- [13] H. E. Rauch, F. Tung., and C. T. Striebel, “Maximum likelihood estimates of linear dynamic systems,” *AIAA Journal*, vol. 3, no. 8, pp. 1445–1450, Aug. 1965.
- [14] A. F. Garcia-Fernandez, L. Svensson, M. R. Morelande, and S. Särkkä, “Posterior Linearization Filter: Principles and Implementation Using Sigma Points,” *IEEE Transactions on Signal Processing*, vol. 63, no. 20, pp. 5561–5573, Oct. 2015.
- [15] M. A. Skoglund, F. Gustafsson, and G. Hendeby, “On Iterative Unscented Kalman Filter using Optimization,” in *Proceedings of the 22nd International Conference on Information Fusion (FUSION)*, Jul. 2019, pp. 1–8.
- [16] A. F. Garcia-Fernandez, L. Svensson, and S. Särkkä, “Iterated Posterior Linearization Smoother,” *IEEE Transactions on Automatic Control*, vol. 62, no. 4, pp. 2056–2063, Apr. 2017.
- [17] F. Tronarp, A. F. Garcia-Fernandez, and S. Särkkä, “Iterative Filtering and Smoothing in Nonlinear and Non-Gaussian Systems Using Conditional Moments,” *IEEE Signal Processing Letters*, vol. 25, no. 3, pp. 408–412, Mar. 2018.
- [18] J. E. Darling and K. J. DeMars, “Minimization of the Kullback–Leibler Divergence for Nonlinear Estimation,” *Journal of Guidance, Control, and Dynamics*, vol. 40, no. 7, pp. 1739–1748, Jul. 2017.
- [19] S. Gultekin and J. Paisley, “Nonlinear Kalman Filtering With Divergence Minimization,” *IEEE Transactions on Signal Processing*, vol. 65, no. 23, pp. 6319–6331, Dec. 2017.
- [20] X. Wang and Z. Ma, “Variational Iterative Filter for Orbit Estimation,” in *Proceedings of the Chinese Automation Congress*. IEEE, Nov. 2019.
- [21] M. D. Vrettas, D. Cornford, and M. Opper, “Estimating parameters in stochastic systems: A variational Bayesian approach,” *Physica D: Nonlinear Phenomena*, vol. 240, no. 23, pp. 1877–1900, Nov. 2011.
- [22] M. D. Vrettas, M. Opper, and D. Cornford, “Variational mean-field algorithm for efficient inference in large systems of stochastic differential equations,” *Physical Review E*, vol. 91, no. 1, Jan. 2015.
- [23] M. D. Vrettas, Y. Shen, and D. Cornford, “Derivations of Variational Gaussian Process Approximation Framework,” Aston University, Tech. Rep., Mar. 2008.

- [24] J. Ala-Luhtala, S. Särkkä, and R. Piché, “Gaussian filtering and variational approximations for Bayesian smoothing in continuous-discrete stochastic dynamic systems,” *Signal Processing*, vol. 111, pp. 124–136, Jun. 2015.
- [25] T. D. Barfoot, J. R. Forbes, and D. J. Yoon, “Exactly sparse Gaussian variational inference with application to derivative-free batch nonlinear state estimation,” *The International Journal of Robotics Research*, 2020.
- [26] J. Nocedal and S. J. Wright, *Numerical Optimization*, 2nd ed. Springer New York, 2006.
- [27] C. Zhang, J. Butepage, H. Kjellström, and S. Mandt, “Advances in Variational Inference,” *IEEE Transactions on Pattern Analysis and Machine Intelligence*, vol. 41, no. 8, pp. 2008–2026, Aug. 2019.
- [28] H. V. Henderson and S. R. Searle, “Vec and vech operators for matrices, with some uses in jacobians and multivariate statistics,” *Canadian Journal of Statistics*, vol. 7, no. 1, pp. 65–81, 1979.
- [29] M. Raitoharju, L. Svensson, A. F. Garcia-Fernandez, and R. Piche, “Damped Posterior Linearization Filter,” *IEEE Signal Processing Letters*, vol. 25, no. 4, pp. 536–540, Apr. 2018.
- [30] S. Särkkä and L. Svensson, “Levenberg–Marquardt and Line-Search Extended Kalman Smoothers,” in *Proceedings of the IEEE International Conference on Acoustics, Speech and Signal Processing (ICASSP)*. IEEE, May 2020.
- [31] M. A. Skoglund, G. Hendeby, and D. Axehill, “Extended Kalman filter modifications based on an optimization view point,” in *Proceedings of the 18th International Conference on Information Fusion (FUSION)*, 2015, pp. 1856–1861.
- [32] E. A. Wan and R. V. D. Merwe, “The unscented Kalman filter for nonlinear estimation,” in *Proceedings of the IEEE Adaptive Systems for Signal Processing, Communications, and Control Symposium*. IEEE, Oct. 2000.
- [33] J. Kokkala, A. Solin, and S. Särkkä, “Sigma-Point Filtering and Smoothing Based Parameter Estimation in Nonlinear Dynamic Systems,” *Journal of Advances in Information Fusion*, 2015.
- [34] J. A. E. Andersson, J. Gillis, G. Horn, J. B. Rawlings, and M. Diehl, “CasADI: a software framework for nonlinear optimization and optimal control,” *Mathematical Programming Computation*, vol. 11, no. 1, pp. 1–36, Jul. 2018.
- [35] MATLAB, *Optimization Toolbox Release 2018b*, The MathWorks, Inc., Natick, Massachusetts, United States, 2018. [Online]. Available: <https://mathworks.com/help/optim/>
- [36] G. Kitagawa, “Non-Gaussian State-Space Modeling of Nonstationary Time Series,” *Journal of the American Statistical Association*, vol. 82, no. 400, p. 1032, Dec. 1987.
- [37] J. W. Tukey, “Some graphic and semigraphic displays,” *Statistical papers in honor of George W. Snedecor*, vol. 5, pp. 293–316, 1972.
- [38] M. K. Pitt and N. Shephard, “Filtering via Simulation: Auxiliary Particle Filters,” *Journal of the American Statistical Association*, vol. 94, no. 446, pp. 590–599, Jun. 1999.
- [39] A. F. Garcia-Fernandez, F. Tronarp, and S. Särkkä, “Gaussian Target Tracking With Direction-of-Arrival von Mises–Fisher Measurements,” *IEEE Transactions on Signal Processing*, vol. 67, no. 11, pp. 2960–2972, Jun. 2019.

A Entropy Decomposition

In this section, the decomposition of I_4 is detailed. This derivation is directly based on [23] with the notation modified to align with the remainder of this paper and relies upon the underlying Markovian nature of state-space

systems.

$$\begin{aligned}
I_4 &= \int q_\beta(x_{0:T}) \log q_\beta(x_{0:T}) dx_{0:T} \\
&= \int q_\beta(x_{0:T}) \log \left(q_\beta(x_0) \prod_{k=0}^{T-1} q_\beta(x_{k+1} \mid x_k) \right) dx_{0:T} \\
&= \int q_\beta(x_{0:T}) \left(\log q_\beta(x_0) + \sum_{k=0}^{T-1} \log q_\beta(x_{k+1} \mid x_k) \right) dx_{0:T} \\
&= \int q_\beta(x_{0:T}) \log q_\beta(x_0) dx_{0:T} \\
&\quad + \sum_{k=0}^{T-1} \int q_\beta(x_{0:T}) \log q_\beta(x_{k+1} \mid x_k) dx_{0:T} \\
&= \int q_\beta(x_{0:T}) \log q_\beta(x_0) dx_{0:T} \\
&\quad + \sum_{k=0}^{T-1} \int q_\beta(x_{0:T}) \log \frac{q_\beta(x_{k+1}, x_k)}{q_\beta(x_k)} dx_{0:T} \\
&= \int q_\beta(x_{0:T}) \log q_\beta(x_0) dx_{0:T} \\
&\quad + \sum_{k=0}^{T-1} \int q_\beta(x_{0:T}) (\log q_\beta(x_{k+1}, x_k) - \log q_\beta(x_k)) dx_{0:T} \\
&= \int q_\beta(x_{0:T}) \log q_\beta(x_0) dx_{0:T} \\
&\quad + \sum_{k=0}^{T-1} \int q_\beta(x_{0:T}) \log q_\beta(x_{k+1}, x_k) dx_{0:T} \\
&\quad - \sum_{k=0}^{T-1} \int q_\beta(x_{0:T}) \log q_\beta(x_k) dx_{0:T} \\
&= \sum_{k=0}^{T-1} \int q_\beta(x_{0:T}) \log q_\beta(x_{k+1}, x_k) dx_{0:T} \\
&\quad - \sum_{k=1}^{T-1} \int q_\beta(x_{0:T}) \log q_\beta(x_k) dx_{0:T} \\
&= \sum_{k=0}^{T-1} \int q_\beta(x_{k:k+1}) \log q_\beta(x_{k+1}, x_k) dx_{k:k+1} \\
&\quad - \sum_{k=1}^{T-1} \int q_\beta(x_k) \log q_\beta(x_k) dx_k.
\end{aligned}$$